### Title
Radiocarbon constraints imply reduced carbon uptake by soils during the 21st century




### Journal
Science, 353(6306)

### ISSN
0036-8075



### Authors
He, Yujie
Trumbore, Susan E
Torn, Margaret S
et al.



### Publication Date
2016-09-23

### DOI
10.1126/science.aad4273

Peer reviewed

# Title: Radiocarbon constraints imply reduced carbon uptake by soils during the 21st century

**Authors:** Yujie He [1]*, Susan E. Trumbore[2], Margaret S. Torn[3], Jennifer W. Harden[4], Lydia J. S. Vaughn[3], Steven D. Allison[1,5], James T. Randerson[1]

**Affiliations:**

[1] Department of Earth System Science, University of California, Irvine, CA, USA

[2] Department of Biogeochemical Processes, Max-Planck-Institute for Biogeochemistry, Jena, Germany

[3] Earth Sciences Division, Lawrence Berkeley National Laboratory, Berkeley, CA, USA

[4] U.S. Geological Survey, Menlo Park, CA, USA

[5] Department of Ecology and Evolutionary Biology, University of California Irvine, Irvine, CA, USA

*Correspondence to: yujie.he@uci.edu

**Subheading:** Reduced carbon uptake by soils during the 21st century

**One Sentence Summary:**

Global radiocarbon observations show that Earth system models, lacking carbon stabilization mechanisms, overestimate the ~~21st century~~ soil carbon sink by almost two-fold.

**Abstract:**

Soil is the largest terrestrial carbon reservoir and may influence the sign and magnitude of carbon cycle-climate feedbacks. ~~Changes in soil carbon—the largest terrestrial carbon reservoir—may influence the sign and magnitude of climate-carbon cycle feedbacks.~~ Many Earth system models (ESMs) estimate a significant soil carbon sink by 2100, yet the underlying carbon dynamics determining this response have not been systematically tested against observations. ~~Using~~ We used $\Delta^{14}C$ data from 157 globally distributed soil profiles sampled to 1 m depth~~, we~~ to show that ESMs underestimated the mean age of soil carbon by more than six-fold (430±50 years vs. 3100±1800 years). Consequently, ESMs overestimated the carbon sequestration potential of soils ~~21st century soil carbon sequestration~~ by nearly two-fold (40 ± 27%). These ~~biases~~inconsistencies suggest that ESMs must better represent carbon stabilization processes and the turnover time of slow and passive reservoirs when simulating future atmospheric $CO_2$ dynamics.

~~To improve simulations of future atmospheric $CO_2$ and carbon storage, ESMs must better represent stabilization processes and turnover times for soil carbon pools.~~

**Keywords:** soil carbon, earth system models, carbon-concentration feedback, mean age, radiocarbon

**Main Text:**

Soil carbon is a dynamic reservoir that may increase substantially in size during the 21st century, as predicted by Earth system models (ESMs), thereby influencing the sign and magnitude of carbon cycle feedbacks under climate change (*1-4*). Under a high radiative forcing scenario (Representative Concentration Pathway 8.5), changes in soil carbon estimated by different models vary from a loss of 20 Pg C to a gain of more than 360 Pg C (*5*). These models suggest that the global carbon inventory in mineral soils may increase by 30% or more over a timespan of about two centuries. The multi-model mean soil carbon accumulation of 109 Pg C (*5*) represents about one decade of global fossil fuel emissions at current rates and 5% of cumulative fossil emissions by 2100 for this scenario (*6*). This soil carbon sink represents a negative feedback on $CO_2$ emissions, and if robust, would slow the rate of climate change.

Still, there are substantial uncertainties in the soil carbon sink projected by ESMs (*5*). Rapid rates of carbon sequestration in ESMs contrast with findings from $CO_2$ and warming experiments (*7, 8*) as well as multiple theoretical and observational constraints indicating slow (millennial) rates of soil organic carbon accrual and turnover (*9-14*). Model uncertainty—as measured by inter-model spread—is high for soil carbon turnover time ($\tau$) and exceeds the uncertainty estimated for carbon uptake through gross primary production (GPP) (*15, 16*).

In coupled model simulations, the relative sink strength (i.e. percentage change in soil carbon) depends on the responses of net primary production (NPP) and soil carbon dynamics to increasing atmospheric $CO_2$ concentrations and to a lesser extent climate change (*5*). Elevated $CO_2$ increases photosynthesis and NPP, which results in greater carbon inputs to soil pools with decadal or longer residence times. Carbon sequestration in soils reduces the build-up of $CO_2$ in the atmosphere (the carbon-concentration feedback). On the other hand, elevated $CO_2$ also

warms the climate, which tends to accelerate soil carbon turnover and reduce carbon storage (the carbon-climate feedback) (*17, 18*). Although these feedbacks oppose one another, the carbon-concentration feedback is more than 4 times greater on average than the carbon-climate feedback in current ESMs at the global scale (*3*). Differences in the representation of elevated $CO_2$ versus climate effects on ecosystem processes result in substantial variation in soil carbon sequestration estimates (*19*) (Table S1).

Without a strong carbon-concentration feedback~~s~~, ESMs would likely project smaller gains or larger losses of soil carbon over the 21$^{st}$ century. Our aim was to constrain the magnitude of the soil carbon-concentration feedback with soil radiocarbon observations. Radiocarbon content ~~can be used to constrain~~provides information about soil carbon turnover over centuries to millennia based on radioactive decay and over decades based on inputs of $^{14}C$ from atmospheric weapons testing ("bomb carbon"). Accurate carbon turnover times are important for ESM projections because pools with short turnover times rapidly adjust to increasing NPP, whereas pools with long turnover times (and by inference low rates of inputs) change only slowly, possibly beyond the time horizon of effective climate mitigation efforts. Therefore inaccuracies in the representation of carbon turnover times will have consequences for the rate and magnitude of the carbon-concentration feedback simulated by ESMs. ~~If ESMs omit soil carbon pools with long turnover times, they could overestimate the carbon-concentration feedback effect on soil carbon storage during the 21$^{st}$ century while underestimating soil carbon storage at steady-state (after millennia).~~

Here we used $\Delta^{14}C$ measurements at 157 sites across multiple biomes (Fig 1, Table S2) along with carbon inventory data to constrain soil carbon dynamics in five biogeochemically-coupled ESM simulations (esmFixClim1) from the Coupled Model Intercomparison Project

Phase 5 (CMIP5) (*20*). In these idealized simulations the atmospheric $CO_2$ mole fraction starts at a preindustrial value of 285 ppm and rises at a rate of 1% $yr^{-1}$, thus quadrupling over 140 yrs. The biogeochemical components of each model experience the increasing trajectory of atmospheric $CO_2$, whereas the atmospheric radiation submodels do not, limiting impacts solely to the direct effects of $CO_2$ on plant physiology and thus enabling diagnosis of carbon-sink sensitivity to increasing $CO_2$.

Total initial soil carbon in the ESMs was not significantly different from the total amount in the top meter of the Harmonized World Soil Database (HWSD; Fig 2a, b) for 4 of the 5 models ($p>0.05$, except CESM $p=0.03$). Therefore we compared ESM-derived $\Delta^{14}C$ to observations derived from soil profiles to a 1 m depth. The carbon and $^{14}C$ patterns of the soil profiles we used were similar to those reported in a recent synthesis paper (*21*), and we used some of the same profiles in our analysis.

Comparing ESM outputs to $^{14}C$ observations requires a model analysis approach because most ESMs do not yet explicitly simulate $\Delta^{14}C$ in soils, and no ESMs had reported turnover times for soil carbon pools. Therefore we used a reduced complexity (RC) model to approximate soil carbon dynamics in each ESM. This approach allowed us to ~~(1)~~ estimate the ~~$^{14}C$ ages and~~ turnover times and $\Delta^{14}C$ associated with the carbon pools in different ESMs (Table S3~~), ). (2) compare with observations, and (3) assess the consequences if ESM parameters were aligned with observations.~~ Where possible, we used a three-pool RC model (with fast, slow, and passive pools) to simulate carbon and $^{14}C$ dynamics. A multi-pool structure is essential because radiocarbon observations show that soil carbon fluxes (NPP inputs and heterotrophic respiration) exchange mainly with short-lived pools whereas carbon stocks are dominated by long-lived pools (*12, 18, 22, 23*). The three-pool RC model had five parameters representing turnover times

of fast, slow, and passive pools ($\tau_{fast}$, $\tau_{slow}$, $\tau_{passive}$) and transfer coefficients ($r_f$ , $r_s$) that regulated carbon flow from the fast to slow, and slow to passive pools (Fig S1). We used a two-pool RC model for GDFL-ESM2M because it represents soil carbon with two pools (*24*) and for HadGEM2-ES because it reported carbon for two pools (Table S4). The two-pool RC model had three parameters, representing $\tau_{fast}$, $\tau_{slow,}$ and $r_f$ (Fig S1). After verifying that the RC model was a good approximation of each ESM based on minimization of root-mean-square error, we used the RC models to simulate $\Delta^{14}C$ values at each grid cell, with observed atmospheric $\Delta^{14}C$~~$^{14}C$~~ for the past 50 kyr as a boundary condition and ~~,~~ accounting for radioactive decay (see supplementary material).

We used an inverse analysis to determine the RC model parameters that were most consistent with our $\Delta^{14}C$ dataset. In the inversion, we ~~held the total carbon mass in the ESM at its preindustrial value (except in sensitivity analyses where it was matched to HWSD observations),~~ ~~and~~ adjusted the parameters described above to match both the total carbon and radiocarbon constraints. With these constraints, turnover time and carbon input rate for each pool were coupled such that an increase in turnover time required a compensatory decline in inputs (Fig S2). RC parameters derived from the inversion were subsequently used to assess consequences of $^{14}C$ constraints for the carbon-concentration feedback.

All ESMs projected an increase in soil carbon over 140 yrs with multi-model mean of 3~~2~~6% (Table 1). This increase was primarily driven by increasing carbon inputs to soil under the quadrupling of $CO_2$ (Table S3), as temperature increased by only a small amount (mean ± 1 s.d. ~~is~~ was 0.52 ± 0.68 °C) for this set of biogeochemically-coupled simulations. CESM showed the smallest soil carbon increase (6.3%) primarily because of low litter inputs relative to other ESMs

(Table S3). For this time period and set of model runs, storage in soil carbon accounted for 42±17% of the total accumulation of carbon in the terrestrial biosphere.

Both two- and three-pool RC models reproduced the global carbon dynamics of the original ESMs (Fig S3-S5; Table S5). The $\tau_{fast}$ across all RC models was less than 20 yrs, while $\tau_{slow}$ varied from 40 to 600 yrs (Fig S6) with a multi-model mean of 212±104 yrs. The mean $\tau_{passive}$ for the three-pool RC models from CESM, IPSL and MRI was 1185±123 yrs (Table 1, Fig S7). Using the RC model parameters estimated at each grid cell within an ESM, we calculated the expected $\Delta^{14}C$. The resulting global average $\Delta^{14}C$ for 1995 (median sample year of site profiles) from the RC models was significantly higher than the mean of the observations (-6.4±64‰ vs. -211±156‰) (Fig 2c,d, $p<0.001$). $\Delta^{14}C$ values from RC models approximating ESMs with passive pools were more negative (-53±35‰) but still significantly higher than the observations ($p<0.001$). Converting these $\Delta^{14}C$ observations into mean age for the soil profile yielded an estimate of 3100±1800 yrs for the observed soil carbon integrated to 1 m and 430±50 yrs for the ESMs (Fig 2e,f). These results indicated that the ESMs did not have enough old carbon that had experienced significant levels of radioactive decay; concurrently the models assimilated too much bomb $^{14}C$. ~~Relative to the observations, the ESM-based RCs underestimated the turnover time of bulk soil carbon and thus assimilated too much bomb $^{14}C$ (and/or had too little old soil carbon that would be depleted in radiocarbon).~~

$^{14}C$-derived mean ages indicate~~s~~ that organic carbon soils is often thousands of years old (*12-14*, *21*), which is an order of magnitude older than suggested by ESM turnover parameters. This discrepancy is likely a consequence of incomplete representation of key biogeochemical processes and difficulties in developing accurate parameterizations for soil carbon at a global scale. Most ESMs do not account for stabilization mechanisms whereby mineral interactions and

aggregate formation protect soil organic matter from decomposition over centuries to millennia (*13, 25-28*). Moreover, first-order decay, as represented in ESMs, may not capture the response of mineral-stabilized carbon to changes in soil moisture, temperature, and other conditions (*29-31*). In addition, some ESM turnover parameters are based on laboratory incubation studies, which are often biased fast compared to *in situ* decomposition rates (*32*). Finally, this set of ESMs did not explicitly resolve vertical differences in soil organic matter dynamics, which may cause underestimation of turnover times in deep soils with large carbon stocks (*21, 25, 33, 34*).

Because the turnover times derived from ESMs were inconsistent with $^{14}C$ observations, we optimized the turnover parameters by fitting our RC models to the observations. We could then run the optimized RC models to re-evaluate ~~21st century~~ soil carbon storage for the transient 1% $yr^{-1}$ simulations. For this inverse approach, we optimized RC model parameters in each grid cell containing an observation site (Fig 2g, 2h, S8, S9). We optimized the τ of the slowest pool and the corresponding transfer coefficient into this pool based on the $-^{14}C$ observations ~~observations~~ while holding soil inputs and τ for the faster pools at their ESM-derived values. The size of the slowest carbon pool was ~~also~~ constrained by optimizing the turnover time and the transfer coefficient together using both $^{14}C$ and total carbon ~~and $^{14}C$~~. Consequently the optimized RC model had about the same total carbon stock as the original ESM, thereby maintaining consistency with carbon inventory data. This optimization approach yielded $\tau_{slow}$ values of 3700±2800 yrs for GFDL and 3500±1300 yrs for HadGEM (using two-pool RC models), which were 16-17 times greater than the turnover times derived from the original ESMs.

For ESMs that included a passive pool, the optimization process yielded three distinct outcomes. For CESM, which has the largest passive pool (73% of soil carbon), the optimized $\tau_{passive}$ was 4500 yrs, which was 3.7±1.5 times greater than $\tau_{passive}$ derived from the original model

(Table 1). IPSL has a smaller fraction of passive carbon (46%) and therefore required a greater $\tau_{passive}$ (16,500 yrs) to obtain agreement with the observed $\Delta^{14}C$. For MRI, the passive pool size was too small (only 13% of soil carbon) to bring $\Delta^{14}C$ into alignment with the profile observations even after parameter optimization (Fig S10, Table S5). To adjust for MRI's potential bias in the passive pool size, we optimized $r_f$ together with $\tau_{passive}$ and $r_s$ to allow for simultaneous changes in slow and passive pool sizes. The resulting RC model for MRI was able to match observations (Fig 2 g,h) with a passive pool fraction of 48% (see Methods; Table S5). These results indicated that increasing the size and turnover time of the passive pool in ESMs would improve agreement with $^{14}C$-based mean age estimates. ~~In general, increasing the size and turnover time of the passive pool in ESMs would improve agreement with $^{14}C$-based age estimates.~~

Bringing turnover time and carbon transfer parameters into agreement with $^{14}C$ observations had significant consequences for the magnitude of the carbon-concentration feedback. Using the $^{14}C$-based parameters, we conducted global transient simulations with each of the five RC models. These simulations showed that the soil as a whole (specifically the slow and passive pools) stored much less carbon in response to increasing levels of atmospheric $CO_2$, primarily as a consequence of reduced flow into the slow or passive pool. The soil carbon sink decreased from 32±18% to 18±12% (Table 1), corresponding to an absolute sink reduction of 170 ± 127 Pg C (Fig 3). ~~Relative to the ESMs, these simulations showed much less soil carbon accumulation in response to increasing levels of atmospheric $CO_2$ because of lower inputs to the slow and/or passive pools. The soil carbon sink decreased from 32±18% to 18±12% (Table 1), corresponding to an absolute sink reduction of 170 ± 127 Pg C (Fig 3).~~ The magnitude of the soil

sink reduction varied widely across the different models; those with larger and older passive fractions at the onset of the transient simulation (Table 1) generally had smaller sink reductions.

To assess the robustness of these sink reductions, we conducted a series of sensitivity experiments (see supplementary material). We found that the sink reduction imposed by constraining the models with $^{14}C$ observations ~~is~~ was robust to (1) turnover times optimized specifically for different biomes; (2) spatial variation and magnitude of ~~in~~ soil carbon stocks; and (3) variations in $\Delta^{14}C$ across measurement sites (Table 2, S6). Sink reductions declined by a factor of 2 when the models were fit to an inventory that was 50% larger than the HSWD dataset, suggesting that if soil carbon pools were larger in ESMs, $^{14}C$-imposed sink reductions would be lower (*35*). Lastly, we used our RC model approach to analyze four fully-coupled ESM runs (1pct$CO_2$) to address potential interactions between the carbon-climate and the carbon-concentration feedback. $^{14}C$ constraints still reduced the sink by at least 40% on average (Fig S11, Table S7) in the fully coupled simulations (see supplementary material).

We conclude that CMIP5 ~~current~~ ESMs underestimated the mean age of soil carbon, especially for slow-cycling pools. By adjusting the turnover times of slow and passive pools to bring the models into alignment with $^{14}C$ observations, the potential for future soil carbon sequestration declined by 40 ± 27%. ~~If turnover times of slow and passive pools are adjusted to bring the ESMs into alignment with $^{14}C$ observations, the potential for 21$^{st}$ century soil carbon sequestration declines by 40±27% in the ESMs we evaluated.~~ Although long-lived soil carbon pools consistent with old $^{14}C$ ages ~~imply~~ imply ~~increased~~ a similar potential for carbon storage at steady state, the timescale required to reach equilibrium is too long to mitigate the potentially damaging climate effects of rising $CO_2$ concentrations during the 21st century (Fig S2). These findings emphasize the need to incorporate $^{14}C$ and other diagnostics into ESM development and

evaluation. In addition, models require better representation of long-term mechanisms of soil carbon stabilization such as organic matter-mineral interactions. Considered together with potential nutrient limitation of NPP inputs to soil (*36*), our analysis suggests that the ~~climate~~carbon-concentration feedback may be weaker in the 21st century than currently expected from ESMs. Therefore a greater fraction of $CO_2$ emissions than previously thought could remain in the atmosphere and contribute to global warming.

## References and Notes:


1. P. Friedlingstein *et al.*, Uncertainties in CMIP5 ~~Climate~~ climate ~~Projections~~ projections due to ~~Carbon~~ carbon ~~Cycle~~ cycle ~~Feedbacks~~feedbacks. *Journal of Climate* **27**, 511-526 (2013).
2. IPCC, *Summary for Policymakers. In: Climate Change 2013: The Physical Science Basis. Contribution of Working Group I to the Fifth Assessment Report of the Intergovernmental Panel on Climate Change*. T. F. Stocker, D. Qin, G.-K. Plattner, M. Tignor, S.K. Allen, J. Boschung, A. Nauels, Y. Xia, V. Bex and P.M. Midgley (eds.), Ed., (Cambridge, United Kingdom and New York, NY, USA., 2013).
3. V. K. Arora *et al.*, Carbon ~~Concentration~~ concentration and ~~Carbon~~carbon ~~Climate~~ climate ~~Feedbacks~~ feedbacks in CMIP5 ~~Earth~~ earth ~~System~~ system ~~Models~~models. *Journal of Climate* **26**, 5289-5314 (2013).
4. C. D. Jones, P. M. Cox, C. Huntingford, Climate-carbon cycle feedbacks under stabilization: Uncertainty and observational constraints. *Tellus B* **58**, 603-613 (2006).
5. K. E. O. Todd-Brown *et al.*, Changes in soil organic carbon storage predicted by ~~Earth~~ earth system models during the 21st century. *Biogeosciences* **11**, 2341-2356 (2014).
6. D. P. Van Vuuren *et al.*, The representative concentration pathways: an overview. *Climatic Change* **109**, 5-31 (2011).
7. J. Lichter *et al.*, Soil carbon sequestration in a pine forest after 9 years of atmospheric $CO_2$ enrichment. *Global Change Biology* **14**, 2910-2922 (2008).
8. W. H. Schlesinger, J. Lichter, Limited carbon storage in soil and litter of experimental forest plots under increased atmospheric $CO_2$. *Nature* **411**, 466-469 (2001).
9. J. W. Harden, R. K. Mark, E. T. Sundquist, R. F. Stallard, Dynamics of soil carbon during deglaciation of the Laurentide ice sheet. *Science* **258**, 1921-1924 (1992).
10. W. H. Schlesinger, Evidence from chronosequence studies for a low carbon-storage potential of soils. *Nature* **348**, 232-234 (1990).
11. B. O'brien, J. Stout, Movement and turnover of soil organic matter as indicated by carbon isotope measurements. *Soil Biology and Biochemistry* **10**, 309-317 (1978).
12. J. B. Gaudinski, S. E. Trumbore, E. A. Davidson, S. H. Zheng, Soil carbon cycling in a temperate forest: radiocarbon-based estimates of residence times, sequestration rates and partitioning of fluxes. *Biogeochemistry* **51**, 33-69 (2000).
13. M. S. Torn, S. E. Trumbore, O. A. Chadwick, P. M. Vitousek, D. M. Hendricks, Mineral control of soil organic carbon storage and turnover. *Nature* **389**, 170-173 (1997).
14. S. E. Trumbore, J. W. Harden, Accumulation and turnover of carbon in organic and mineral soils of the BOREAS northern study area. *Journal of~~.~~ Geophy~~s~~sical~~.~~ Research~~.~~* **102**, 28817-28830 (1997).
15. N. Carvalhais *et al.*, Global covariation of carbon turnover times with climate in terrestrial ecosystems. *Nature* **514**, 213-217 (2014).
16. A. D. Friend *et al.*, Carbon residence time dominates uncertainty in terrestrial vegetation responses to future climate and atmospheric $CO_2$. *Proceedings of the National Academy of Sciences* **111**, 3280-3285 (2014).
17. X. Wang *et al.*, Soil respiration under climate warming: differential response of heterotrophic and autotrophic respiration. *Global Change Biology* **20**, 3229-3237 (2014).
18. W. Knorr, I. C. Prentice, J. I. House, E. A. Holland, Long-term sensitivity of soil carbon turnover to warming. *Nature* **433**, 298-301 (2005).
19. C. D. Koven *et al.*, Controls on terrestrial carbon feedbacks by productivity vs. turnover in the CMIP5 Earth System Models. *Biogeosciences ~~Discuss.~~* **12**, ~~5757-5801~~5211-5228 (2015).
20. K. E. Taylor, R. J. Stouffer, G. A. Meehl, An overview of CMIP5 and the experiment design. *Bulletin of the American Meteorological Society* **93**, 485-498 (2012).

27421. J. A. Mathieu, C. Hatté, J. Balesdent, É. Parent, Deep soil carbon dynamics are driven more by
275 soil type than by climate: a worldwide meta-analysis of radiocarbon profiles. *Global Change*
276 *Biology* **21**, 4278-4292 (2015).
27722. S. Trumbore, Age of ~~Soil~~ soil ~~Organic~~ organic ~~Matter~~ matter and ~~Soil~~ soil ~~Respiration~~respiration:
278 ~~Radiocarbon~~ radiocarbon ~~Constraints~~ constraints on ~~Belowground~~ belowground ~~Carbon~~ carbon
279 ~~Dynamics~~dynamics. *Ecological Applications* **10**, 399-411 (2000).
28023. W. Feng et al., Methodological uncertainty in estimating carbon turnover times of soil fractions.
281 *Soil Biology and Biochemistry* **100**, 118-124 (2016).
28224. E. Shevliakova *et al.*, Carbon cycling under 300 years of land use change: Importance of the
283 secondary vegetation sink. *Global Biogeochemical Cycles* **23**, (2009).
28425. M. W. Schmidt *et al.*, Persistence of soil organic matter as an ecosystem property. *Nature* **478**, 49-
285 56 (2011).
28626. M. v. Lützow *et al.*, Stabilization of organic matter in temperate soils: mechanisms and their
287 relevance under different soil conditions~~ –a~~ review. *European Journal of Soil Science* **57**, 426-445
288 (2006).
28927. J. A. Dungait, D. W. Hopkins, A. S. Gregory, A. P. Whitmore, Soil organic matter turnover is
290 governed by accessibility not recalcitrance. *Global Change Biology* **18**, 1781-1796 (2012).
29128. M. Kleber, R. Mikutta, M. S. Torn, R. Jahn, Poorly crystalline mineral phases protect organic
292 matter in acid subsoil horizons. *European Journal of Soil Science* **56**, 717-725 (2005).
29329. J. S. Clemente, A. J. Simpson, M. J. Simpson, Association of specific organic matter compounds
294 in size fractions of soils under different environmental controls. *Organic Geochemistry* **42**, 1169-
295 1180 (2011).
29630. C. Koven *et al.*, The effect of vertically resolved soil biogeochemistry and alternate soil C and N
297 models on C dynamics of CLM4. *Biogeosciences* **10**, 7109-7131 (2013).
29831. B. Ahrens, M. C. Braakhekke, G. Guggenberger, M. Schrumpf, M. Reichstein, Contribution of
299 sorption, DOC transport and microbial interactions to the $^{14}C$ age of a soil organic carbon profile:
300 Insights from a calibrated process model. *Soil Biology and Biochemistry* **88**, 390-402 (2015).
30132. G. B. Bonan, M. D. Hartman, W. J. Parton, W. R. Wieder, Evaluating litter decomposition in earth
302 system models with long-term litterbag experiments: an example using the Community Land
303 Model version 4 (CLM4). *Global Change Biology* **19**, 957-974 (2013).
30433. C. R. Lawrence, J. W. Harden, X. Xu, M. S. Schulz, S. E. Trumbore, Long-term controls on soil
305 organic carbon with depth and time: A case study from the Cowlitz River Chronosequence, WA
306 USA. *Geoderma* **247**, 73-87 (2015).
30734. C. Rumpel, I. Kögel-Knabner, Deep soil organic matter—a key but poorly understood component
308 of terrestrial C cycle. *Plant and Soil* **338**, 143-158 (2011).
30935. Y. Luo *et al.*, Toward more realistic projections of soil carbon dynamics by Earth system models.
310 *Global Biogeochemical Cycles* **30**, 40-56 (2016).
31136. W. R. Wieder, C. C. Cleveland, W. K. Smith, K. Todd-Brown, Future productivity and carbon
312 storage limited by terrestrial nutrient availability. *Nature Geoscience* **8**, 441-U435 (2015).

**Acknowledgments:**

We thank ~~Lesego Khomo and Oliver Chadwick for use of unpublished data and~~ **C. Hatté** for sharing her compilation of published $^{14}C$ profiles. We received funding support from the Climate and Environmental Sciences Division of Biological and Environmental Research (BER) in the U.S. Department of Energy Office of Science. This included support from the Regional and Global Climate Modeling Program to the Biogeochemical Cycles Feedbacks Science Focus Area and several grants from the Terrestrial Ecosystem Science Program (DESC0014374 and DE-AC02-05CH11231). ~~This study was supported by the U.S. Department of Energy, Office of Science, Office of Biological and Environmental Research, Regional and Global Climate Modeling (Biogeochemical Cycles Feedbacks Science Focus Area) and Terrestrial Ecosystem Science (DESC0014374 and contract DE-AC02-05CH11231) Programs in the Climate and Environmental Sciences Division of Biological and Environmental Research (BER) in the U.S. Department of Energy Office of Science.~~ The model simulations analyzed in this study were obtained from the Earth System Grid Federation CMIP5 online portal hosted by the Program for Climate Model Diagnosis and Intercomparison at Lawrence Livermore National Laboratory (https://pcmdi.llnl.gov/projects/esgf-llnl/).

**Table 1:** Global soil carbon stocks and carbon uptake for CMIP5 models that experienced a quadrupling of atmospheric $CO_2$ from a preindustrial value of 285 ppm over a period of 140 years.

| ESM | Initial SOC (Pg C) | % change in SOC | % change in SOC after $^{14}C$ constraint | $^{14}C$- imposed sink reduction (%) | $\tau^{slow}$ (yr)1 | $\tau_{passive}$ (yr) | $r_f$ | $r_s$ | $^{14}C$- imposed correction factors[2] | | | |
|---|---|---|---|---|---|---|---|---|---|---|---|---|
| | | | | | | | | | $\tau_{slow}$ | $\tau_{passive}$ | $r_f$ | $r_s$ |
| CESM1(BGC) | 571 | 6.3 | 5.1 | 19 | 56±16 | 1310±241 | 0.06±0.05 | 0.33±0.05 | - | 3.7±1.5 | - | 0.34±0.75 |
| GFDL-ESM2M | 1344 | 26 | 3.3 | 87 | 231±196 | - | 0.17±0.07 | - | 16±18 | - | 0.06±0.14 | - |
| HadGEM2-ES | 1028 | 63 | 33 | 46 | 208±84 | - | 0.12±0.07 | - | 17±12 | - | 0.07±0.32 | - |
| IPSL-CM5A-LR | 1340 | 27 | 25 | 5.9 | 218±82 | 1181±347 | 0.06±0.03 | 0.29±0.07 | - | 14±8.3 | - | 0.07±0.14 |
| MRI-ESM1[3] | 1403 | 36 | 22 | 40 | 347±117 | 1065±257 | 0.17±0.09 | 0.10±0.06 | - | 13±7.2 | 0.46±0.79 | 0.34±0.74 |
| **Mean**[4] | **1137**±312 | **32**±18 | **18**±12 | **40**±27 | **212**±104 | **1185**±123 | **0.12**±0.06 | **0.24**±0.12 | **16.5**±0.5 | **10.2**±4.6 | - | - |

[1] $\tau_{slow}$, $\tau_{passive}$ denote the turnover time, and $r_f$, $r_s$ denote the transfer coefficient from the fast to the slow pool, and from the slow to the passive pool respectively. Reported values were estimated as an area-weighted mean and standard deviation of all model grid cells.

[2] The mean and standard deviation of the $^{14}C$-imposed correction factors were derived from using the $^{14}C$ observations at each site in a single optimization, and then averaging these scalar adjustments across the set of 157 optimizations.

[3] The $^{14}C$-constrained sink reduction and correction factor for MRI were based on an inverse analysis that changed the pool size of both slow and passive pools. The reported percent change in SOC and sink reduction were derived from transient simulations starting at steady state with the reduced complexity model. See methods in supporting material.

[4] The multi-model mean and standard deviation were estimated using the mean value from each of the 5 ESMs.

**Table 2:** Summary of sensitivity experiments.

| Experiment | % change in SOC after $^{14}C$ constraint[1] | $^{14}C$- imposed sink reduction (%)[1] | Correction factor for turnover time[1] | Correction factor for transfer coefficient[1] |
|---|---|---|---|---|
| Biome-specific inversions | 17±11 | 43±24 | - | - |
| Match SOC with HWSD at sites[2] | 18±12 | 31±40 | 13±4.5 | 0.19±0.23 |
| Match SOC with 1.5*HWSD at sites[2] | 21±12 | 19±42 | 11±4.5 | 0.38±0.39 |
| -1 S.D. of inter-site variation | 14±9.9 | 52±23 | - | - |
| +1 S.D. of inter-site variation | 23±16 | 25±25 | - | - |

[1] The mean and standard deviation were estimated from the global mean change of each of the 5 individual ESMs. The correction factors for the turnover time and transfer coefficients are reported for the slowest carbon pool.

[2] The correction factors were obtained at each site, and then the mean scalar across all sites was applied to the global forward simulation.

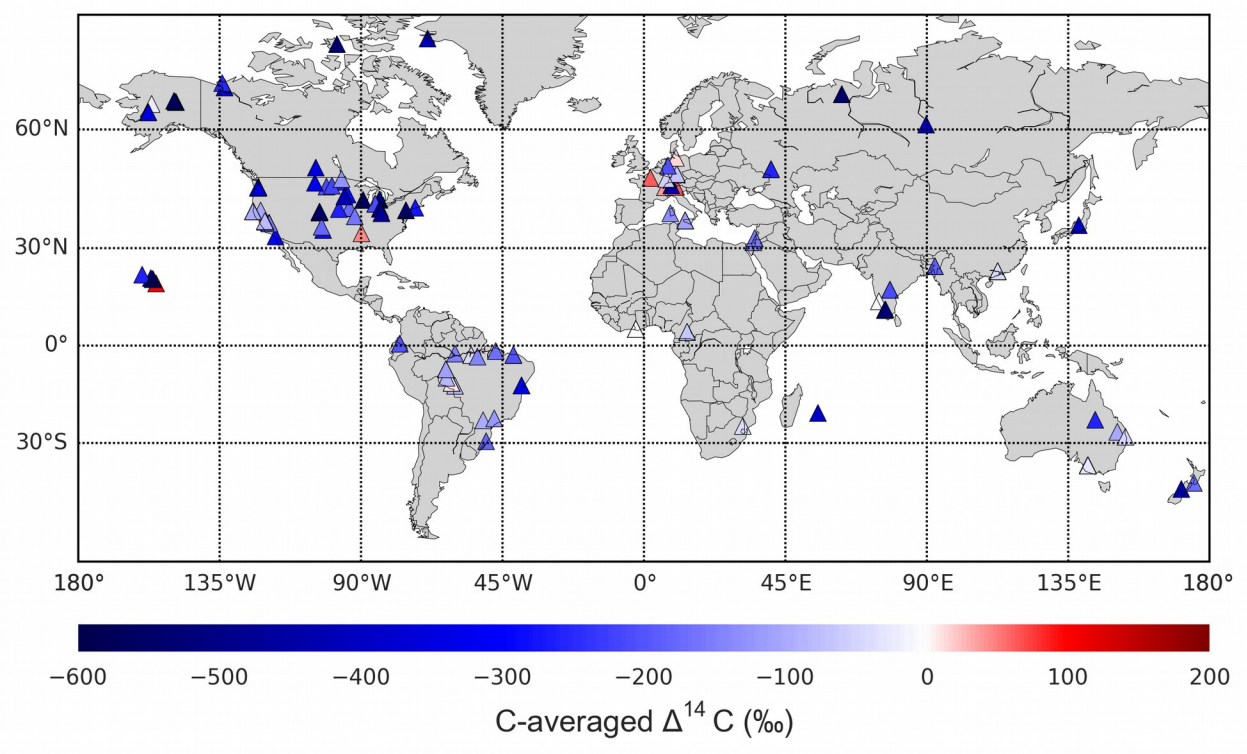


**Fig 1:** Location of radiocarbon soil profiles used to constrain ESM soil carbon mean ages and turnover times (N=157). The carbon-weighted $\Delta^{14}C$ to a depth of 1m is denoted with the color shade of each symbol. A summary of the location, sample year, and reference for each site is provided in Table S2.

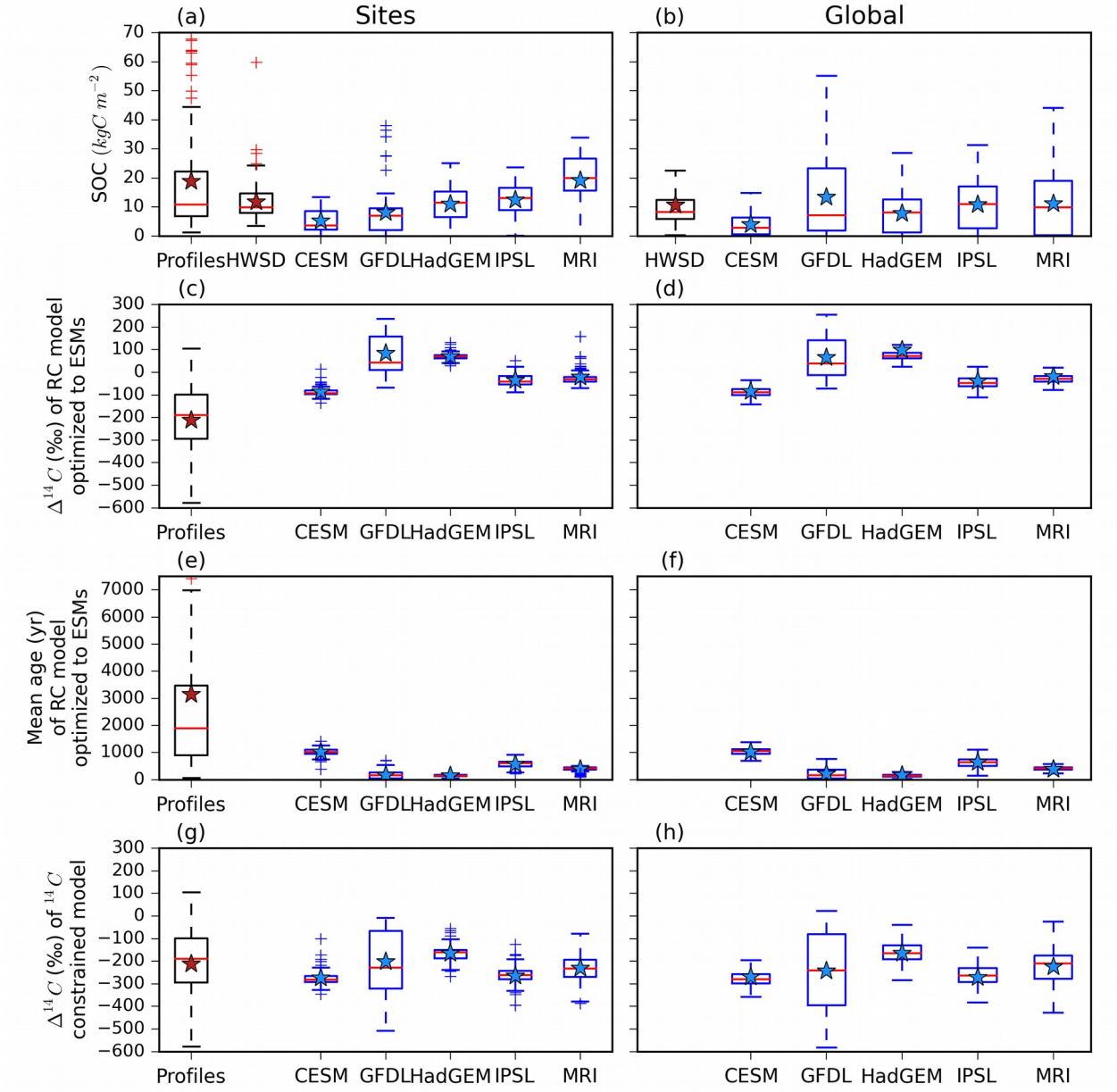


355

356**Fig 2:** Soil organic carbon content (a, b) of the original ESMs, $\Delta^{14}C$ of the reduced complexity
357model optimized to the original ESMs (c, d), corresponding mean age (e, f), and the $\Delta^{14}C$ of the
358$^{14}C$-constrained reduced complexity models (g, h). Left column shows the values of the models
359sampled at the locations of the individual soil profiles; right column shows the global model
360distribution. Data from profile sites and the Harmonized World Soil Database represent carbon

content in the top 1 m of soil; data from ESMs are the total carbon stock. Star denotes the mean; the '+' symbol denotes outliers beyond the 25th and 75th percentiles.

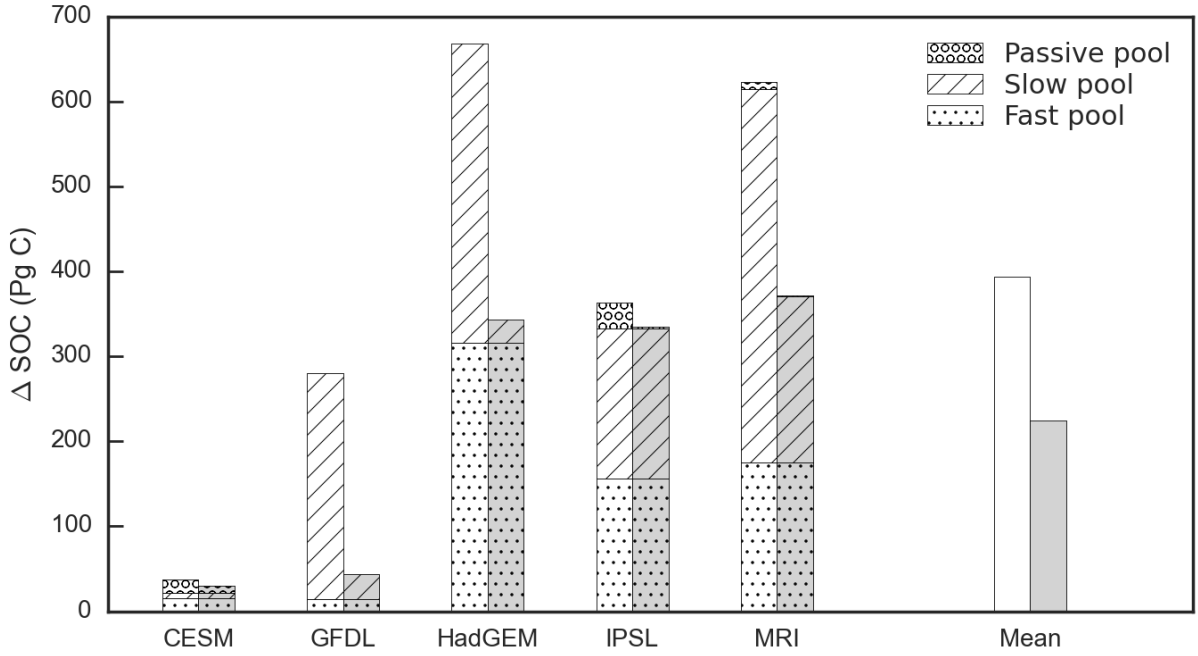


**Fig 3:** Absolute change in SOC content from the reduced complexity model fit to the original ESM (bars with white background) and the estimate obtained by applying the $^{14}C$ constraint to the reduced complexity model (bars with gray background). The estimates on the right side show the total carbon content (sum of fast, slow, and passive) averaged across all the models, before and after applying the radiocarbon constraint.

**Supplementary Materials:**

Materials and Methods

Sensitivity Analysis Results

Fully-Coupled Simulation Analysis

Figures S1-S11

Tables S1-S7

References 37-110